

1 **Sporulation-specific cell division defects in *yImE* mutants of *Streptomyces coelicolor* are**
2 **rescued by additional deletion of *yImD***

3

4 Le Zhang¹, Joost Willemse¹, Paul A. Hoskisson² and Gilles P. van Wezel^{1,*}

5

6

7 ¹ *Molecular Biotechnology, Institute of Biology, Leiden University, Sylviusweg 72, 2333 BE, The*
8 *Netherlands*

9 ² *Strathclyde Institute of Pharmacy and Biomedical Science, University of Strathclyde, 161*
10 *Cathedral Street, Glasgow, G4 0RE, United Kingdom*

11

12

13 * Author for correspondence. Tel: +31 71 5274310; email: g.wezel@biology.leidenuniv.nl.

14

15

16

17

18

19

20

21

22

23

24 **ABSTRACT**

25 Cell division during the reproductive phase of the *Streptomyces* life-cycle requires tight
26 coordination between synchronous formation of multiple septa and DNA segregation. One
27 remarkable difference with most other bacterial systems is that cell division in *Streptomyces* is
28 positively controlled by the recruitment of FtsZ by SsgB. Here we show that deletion of *yldM*
29 (SCO2081) or *yldE* (SCO2080), which lie in operon with *ftsZ* in the *dcw* cluster of actinomycetes,
30 has major consequences for sporulation-specific cell division in *Streptomyces coelicolor*.
31 Electron and fluorescence microscopy demonstrated that *yldE* mutants have a highly aberrant
32 phenotype with defective septum synthesis, and produce very few spores with low viability and
33 high heat sensitivity. FtsZ-ring formation was also highly disturbed in *yldE* mutants. Deletion of
34 *yldM* had a far less severe effect on sporulation. Interestingly, the additional deletion of *yldM*
35 restored sporulation to the *yldE* null mutant. YldM and YldE are not part of the divisome, but
36 instead localize diffusely in aerial hyphae, with differential intensity throughout the sporogenic
37 part of the hyphae. Taken together, our work reveals a function for YldM and YldE in the
38 control of sporulation-specific cell division in *S. coelicolor*, whereby the presence of YldM alone
39 results in major developmental defects.

40

41

42 **INTRODUCTION**

43 In unicellular bacteria, cell division divides a mother cell in two identical daughter cells, each
44 containing a single copy of the chromosome. The control of cell division thereby revolves
45 around finding the mid-cell position, and chromosome segregation and septum synthesis are
46 closely coordinated in time and space to avoid DNA damage by the nascent septum. The cell
47 division scaffold is formed by FtsZ, which is a homologue of tubulin¹ and forms a contractile ring
48 (or Z-ring) that mediates the recruitment of the cell division machinery to the division site
49 (reviewed in^{2,3}). Septum-site selection and Z-ring stabilization are mediated by proteins like
50 FtsA and ZipA⁴⁻⁶, ZapA⁷ and SepF^{8,9}. Z-ring (dis-)assembly is thereby actively controlled
51 (reviewed in¹⁰).

52 Streptomyces are filamentous Gram-positive bacteria that belong to the phylum of
53 Actinobacteria. These bacteria produce over 60% of all known antibiotics and many other
54 bioactive natural products^{11,12}. Exponential growth of the vegetative hyphae is achieved by
55 apical growth and branching. At this stage of the life cycle, cell division does not affect physical
56 separation of the cells, but instead long syncytial cells are formed that are separated by cross-
57 walls¹³. Hence, streptomyces are model organisms for the study of multicellularity and
58 bacterial morphogenesis^{14,15}.

59 Most divisome components except FtsZ are not required for vegetative division,
60 presumably reflecting the lack of constriction¹⁶. Spacing between the cross-walls is highly
61 variable, and little is known of the way septum-site selection is controlled. Recently, using cryo-
62 electron tomography, our lab and others showed that intracellular membrane assemblies or
63 cross-membranes are involved in DNA protection during septum synthesis in young vegetative

64 hyphae, suggesting a novel way of cell-division control ^{17,18}. In addition, these multicellular
65 bacteria have a complex cytoskeleton, which among others plays a role in the organization of
66 the tip growth machinery ^{19,20}.

67 Canonical division resulting in cell fission occurs during sporulation-specific cell division,
68 which requires all components of the divisome ^{16,21}. At this stage of the life cycle up to a
69 hundred septa are formed in a short time span, following a highly complex process of
70 coordinated cell division and DNA segregation, and visualized as long ladders of Z-rings ²².
71 Eventually, chains of unigenomic spores are formed, which have a thick protective spore wall
72 facilitating long-term survival in the environment. Though *ftsZ* null mutants are viable, they fail
73 to produce septa and hence do not sporulate, cell division is not essential for growth of
74 *Streptomyces*, which provides a unique system for the study of this process ^{23,24}.

75 Sporulation-specific cell division is controlled by the SsgA-like proteins (SALPs), which are
76 exclusively found in morphologically complex actinobacteria ^{25,26}. The canonical view is that cell
77 division is negatively controlled by the action of the Min system that inhibits division away from
78 midcell, and by nucleoid occlusion (Noc) to avoid septum synthesis near the chromosome to
79 avoid DNA damage, as seen in *B. subtilis* and *E. coli*. In contrast, cell division in streptomycetes is
80 positively controlled by the recruitment of FtsZ to future septum sites by SsgB, in an SsgA-
81 dependent manner ²⁷. As a consequence, both SsgA and SsgB are required for sporulation ^{28,29}.
82 We recently showed that SepG (formerly called YlmG) assists in docking of SsgB to the
83 membrane, and also plays a major role in maintaining the nucleoid shape in the spores ³⁰.

84 Many of the genes for the components of the divisome and the cell-wall biosynthetic
85 machinery are located in the so-called *dcw* cluster (division and cell-wall synthesis; ³¹). Most of

86 these genes have been studied extensively and their functions have been well characterized.
87 However, little is known of the genes *yImD* and *yImE* that lie immediately downstream of, and
88 likely form an operon with, *ftsZ* on the genome of streptomycetes and many other bacteria,
89 including firmicutes. Earlier work on a mutant of *S. venezuelae* lacking both *yImD* and *yImE*
90 showed that the double mutant had no obvious phenotypic defects³².

91 In this study, we show that deletion of *yImE* alone results in severe cell division defects,
92 while deletion of *yImD* only slightly affects sporulation. Interestingly, the cell division defects of
93 *yImE* mutants were rescued by the additional deletion of *yImD*, and *yImDE* mutants had no
94 obvious sporulation defects. These data strongly suggest that expression of YImD alone is
95 detrimental for sporulation-specific cell division in streptomycetes, which is counteracted by
96 YImE. This is consistent with the phylogenetic evidence that some bacteria only harbor an
97 ortholog of *yImE*, whereas *yImD* never occurs without *yImE*.

98

99 **RESULTS & DISCUSSION**

100

101 **Phylogenetic analysis of YlmE (SCO2080) and YlmD (SCO2081)**

102 Many of the genes in the *dcw* gene cluster have been extensively studied and their functions are
103 well established. However, this is not the case for *yldM* and *yldE*, which lie immediately
104 downstream of *ftsZ* in many bacteria. In all *Streptomyces* genomes analyzed, *ftsZ* (SCO2082),
105 *yldM* (SCO2081) and *yldE* (SCO2080) form an operon, an observation that is supported by high-
106 resolution transcript mapping ³³; moreover there is apparent translational fusion between *ftsZ*
107 and *yldM* (overlapping start and stop codons) and only 6 nt spacing between *yldM* and *yldE*.
108 This transcriptional coupling to *ftsZ* suggests that these genes may play a prominent role in the
109 cell division process. Transcript levels of *ftsZ* are similar to those of *yldM* and *yldE* during
110 vegetative growth on MM agar plates; however, transcription of *ftsZ* is enhanced during
111 sporulation, while that of *yldM* and *yldE* is not significantly altered ³⁴. YldM and YldE are wide-
112 spread in Gram-positive bacteria, and particularly in actinobacteria. SCO2081 and SCO2080
113 share 32% aa identity with YldM and YldE of *B. subtilis*, respectively. Orthologues of these
114 proteins are also found in several genera of Gram-negative bacteria. Phylogenetic analysis of
115 the YldM and YldE proteins in actinobacteria shows that while YldE is widespread, YldM is
116 often absent in actinobacteria, such as *Stackebrandtia*, *Catenulispora*, *Salinispora*,
117 *Micromonospora*, *Amycolatopsis* and *Mycobacterium*, several of which are spore-forming
118 actinobacteria (Fig. 1). Remarkably, there are no examples of *yldM* being present in the absence
119 of *yldE* and thus it would appear that loss of YldM (SCO2081) has occurred on multiple
120 occasions, given that there is wide but patchy distribution of this gene across distinct

121 actinobacteria lineages and the sequences clade tightly within the accepted actinomycete
122 phylogenies.

123 Analysis of *yldM* using the EMBL String engine ³⁵ shows functional linkage in two groups
124 to cell division associated genes (*sepF* (SCO2079), SCO2085 and *ftsZ*) along with a group of
125 mainly hypothetical proteins (STRING Data link: <http://bit.ly/2gc5kCB>). *YldM* has a domain that
126 has homology to the multiple-copper polyphenol oxidoreductase laccases, which are
127 oxidoreductases that are widely distributed in both prokaryotes and eukaryotes ³⁶. A similar
128 analysis of *YldE* also indicates a functional linkage to cell-wall biosynthesis and cell division
129 (STRING Data link: <http://bit.ly/2gbPyHK>). *YldE* is a member of the family of YBL036c-like
130 proteins, which generally contain pyridoxal 5-phosphate dependent enzymes. The structure of
131 YBL036c from *Saccharomyces cerevisiae* was resolved at 2.0 Å resolution (PDB 1CT5,³⁷). The
132 protein has homology to the N-terminal domains of alanine racemases but lacks of the β-
133 sandwich domain which would likely limit the activity of YBL036c as alanine or non-specific
134 amino acid racemase ³⁸. To test the hypothesis that *YldE* may have alanine racemase activity
135 and thus may play a role in determining the amino acid composition of the peptidoglycan, we
136 tested purified *YldE* for alanine racemase assays as described previously ³⁹, using alanine
137 racemase *Alr* as positive control. Whereas purified *Alr* successfully catalyzed the conversion of L-
138 alanine to D-alanine, *YldE* could not perform this reaction under the same conditions, and over-
139 expression of *YldE* failed to restore a D-Ala prototrophy to *alr* null mutants (data not shown).
140 These observations coupled with protein structure homology data make it highly unlikely that
141 *YldE* functions as an alanine racemase *in vivo*.

142

143 ***yImD* and *yImE* are required for proper sporulation**

144 To analyze the role of *yImD* and *yImE*, deletion mutants were created in *S. coelicolor* M145 as
145 detailed in the Materials and Methods section. The +25 to +696 region of *yImE* (SCO2080) or the
146 +25 to +705 region of *yImD* (SCO2081) were replaced by the apramycin resistance cassette,
147 followed by deletion of the cassette using the Cre recombinase so as to avoid polar effects. For
148 each mutant, four independent mutants were selected and all had the same phenotype.
149 Therefore, one was selected for more detailed analysis, designated GAL47 (*S. coelicolor* M145
150 Δ *yImD*) and GAL48 (*S. coelicolor* M145 Δ *yImE*). The M145 *yImDE* mutant (GAL130) was created
151 by replacing *yImD* in *yImE* null mutant GAL48 by the apramycin resistance cassette.

152 The *yImD* null mutant GAL47 had a wild-type-like appearance, while *yImE* null mutant
153 GAL48 hardly produced any grey pigment after 5 days incubation on SFM agar plates, indicative
154 of a failure to complete full development. Surprisingly, *yImDE* mutant GAL130 had a grey
155 appearance similar to that of the parental strain M145 (Fig. 2A). Phase-contrast light microscopy
156 of impression prints of the top of the colonies demonstrated that while the parent produced
157 typical long spore chains, the *yImD* null mutant produced abundant but aberrantly sized spores,
158 the *yImE* null mutant produced fewer spores and those produced were unusually large. The
159 *yImDE* double mutant produced abundant spores, though some were irregularly sized (Fig. 2B
160 and Fig. S1). The same defect in sporulation was observed on R5 and MM mannitol agar plates.
161 Antibiotic production was not affected, and the mutants produced normal levels of the
162 pigmented antibiotics actinorhodin and undecylprodigiosin.

163 To further ascertain that the sporulation defects were indeed solely due to the deletion
164 of the respective genes, we introduced plasmids expressing *yImD* or *yImD-egfp* in the in the

165 *yImD* null mutant and *yImE* or *yImE-egfp* in the *yImE* mutant, in all cases with transcription
166 directed from the native *ftsZ* promoter region. While the majority of the spores of the
167 complemented *yImD* mutant had a regular appearance, those of the complemented *yImE*
168 mutants still showed variable lengths (Fig. 2B). This partial complementation suggests that the
169 deletion of *yImE* may have polar effect on the expression of its downstream genes. This is
170 supported by the fact that introduction of a plasmid harboring the entire region from *murD* to
171 *divIVA* fully restored sporulation to *yImE* mutants (Fig 2B & Fig. S2). Promoter probing using the
172 *redD* reporter system ⁴⁰ showed that besides the intergenic promoter between *yImE* and *sepF*,
173 an additional promoter is located within *yImE*, suggesting that deletion of the entire *yImE* gene
174 negatively affects the transcription of *sepF* (data not shown). This may explain why *yImE* alone
175 failed to fully complement the *yImE* null mutant.

176 To quantify the spore lengths and their size distribution (*i.e.* variability), approximately 300
177 spores from the parental strain *S. coelicolor* M145, its *yImD* and *yImE* mutants and the
178 genetically complemented strains were measured from light images from phase-contrast
179 microscopy (100x magnification). Spore sizes were compared using a boxplot analysis (Fig. 2C).
180 Wild-type spores typically had lengths between 0.8-1.2 μ m, with an average length of $1.01 \pm$
181 0.15 μ m, while *yImD* mutant spores showed a slightly broader distribution (Fig. 2C), with an
182 average length of 1.12 ± 0.27 μ m. The average length was reduced to wild-type levels by
183 complementation, namely to 1.03 μ m and 1.05 μ m by introduction of *yImD* and *yImD-egfp*,
184 respectively. Spores of the *yImE* null mutant were much larger and with a significantly wider
185 variation, showing an average length of 2.23 ± 0.86 μ m (Fig. 2C). Genetic complementation of
186 the *yImE* mutant restored spore length variation of *yImE* mutant to wild-type levels, with an

187 average size of 1.03 ± 0.19 μm . Partial complementation of the *yImE* null mutant was seen when
188 constructs expressing *yImE* or *yImE-egfp* were introduced into the mutant, with spore lengths of
189 1.62 ± 0.50 μm and 1.85 ± 0.59 μm , respectively. The average spore length of the combined
190 *yImDE* mutant was much closer to that of the parental strain, namely 1.23 ± 0.34 μm , thereby
191 showing significantly smaller size variation than *yImE* null mutants (Fig. 2C). The statistical
192 validity of the variations in spore sizes between mutants and the parental strain was validated
193 by a Kolgomorov-Smirnov test and a Mann-Whitney U test, which confirmed that the sizes of
194 mutant spores deviated significantly from those of wild-type spores.

195 To study the spores of *yImD* and *yImE* null mutants at high resolution, cryo-scanning
196 electron microscopy (SEM) was performed, which again demonstrated the sporulation defects.
197 The parental strain *S. coelicolor* M145 produced abundant spore chains, with nearly all hyphae
198 fully developed into mature spore chains (Fig. 3AB). The *yImD* null mutant GAL47 frequently
199 produced aberrantly sized spores (Fig. 3CD), while in *yImE* null mutant GAL48, precious few and
200 often aberrant spores were identified (Fig. 3EF). The same approach was used to create *yImD*
201 and *yImE* mutants in *Streptomyces lividans* 66, and these again showed the same morphology,
202 strongly supporting the notion that the observed phenotypes were solely due to the mutations
203 in *yImD* or *yImE* (data not shown). The highly similar phenotypes of the *S. coelicolor* and *S.*
204 *lividans* mutants support the notion that the genes play a key role in sporulation-specific cell
205 division and are consistent with the conserved function of the genes in sporulation-specific cell
206 division in *Streptomyces*.

207

208 **Deletion of *yImD* and especially *yImE* results in reduced robustness of spores**

209 Viability of the spores was tested by plating around 1000 spores - counted in a hemocytometer -
210 of *S. coelicolor* M145 and its mutants GAL47 ($\Delta ylmD$) and GAL48 ($\Delta ylmE$) onto SFM agar plates.
211 While the wild-type strain had close to 100% viability, spores of the $ylmD$ and $ylmE$ mutants had
212 reduced viability, with 50% and 60% viable spores, respectively. Spores of in particular the $ylmE$
213 mutant were heat sensitive, with only $11 \pm 1\%$ viability after 15 min incubation at 58^0C , as
214 compared to $47 \pm 6\%$ survival for $ylmD$ null mutant spores and $55 \pm 5\%$ for the parental strain.
215 Genetic complementation of the $ylmE$ null mutant restored wild-type survival to heat shock (58
216 $\pm 3\%$). The same was true when $ylmD$ was deleted in the $ylmE$ null mutant ($56 \pm 4\%$ survival).

217 To analyze the possible cell-wall defects in more detail, all strains were grown on SFM
218 agar plates for 5 days and analyzed by Transmission Electron Microscopy (TEM) (Fig. 4). The
219 parent produced typical spore chains and thick-walled spores. Conversely, $ylmD$ and $ylmE$
220 mutant spores were deformed and highly irregular. In particular the spores of the $ylmE$ mutant
221 had a thin wall similar to that of hyphae, suggesting that spore-wall synthesis was compromised.

222

223 **YlmD and YlmE are required for peptidoglycan synthesis at the septum**

224 To analyze cell wall and membrane distribution in $ylmD$ and $ylmE$ mutants, fluorescence
225 microscopy was performed on five-days old SFM surface-grown cultures of mutants GAL47
226 (M145 $\Delta ylmD$) and GAL48 (M145 $\Delta ylmE$) and compared to the parental strain M145.
227 Peptidoglycan precursors were stained with FITC-WGA or Oregon-WGA and membranes
228 visualized by staining with FM5-95. In wild-type pre-division aerial hyphae, long symmetrical
229 septal ladders were observed when stained for cell wall or membranes (Fig. 5A). In contrast,
230 aerial hyphae of the mutants showed highly disturbed cell wall and membrane distribution,

231 which was more pronounced in *yImE* than in *yImD* mutants (Fig. 5A). Septation of *yImD* mutants
232 was complemented via re-introduction of *yImD*; similarly, septation was restored to the *yImE*
233 mutant by re-introduction of *yImE*, although peptidoglycan synthesis and septum spacing was
234 still irregular (Fig. 5B). These data again show that the consequences of deleting *yImE* are much
235 more severe for sporulation-specific cell division than when *yImD* is deleted.

236

237 **Cellular localization of YImD and YImE**

238 Given the impact of *yImDE* on sporulation, we analyzed how YImD and YImE were localized in
239 the hyphae of *S. coelicolor*. To this end, constructs based on the low-copy number vector
240 pHJL401 were prepared to allow the expression of YImD-eGFP and YImE-eGFP fusion proteins,
241 which were expressed from the natural *ftsZ* promoter region (see Materials and Methods
242 section for details). These constructs were then introduced into *S. coelicolor* M145 and (as a
243 control for functionality) in the mutants. The constructs partially restored development to the
244 respective mutants, with significant restoration of the sporulation defects in *yImD* mutants, and
245 partial restoration of sporulation to *yImE* mutants (Fig. 2B).

246 In vegetative hyphae, only very weak signals were obtained for YImD-eGFP and YImE-
247 eGFP, indicative of low protein expression (Fig. 6A). In early and late aerial hyphae, both YImD-
248 eGFP and YImE-eGFP became more visible and showed diffuse localization along the wall of the
249 aerial hyphae (Fig. 6A). During early sporulation, YImD-eGFP and YImE-eGFP showed an irregular
250 pattern of varying intensity, with some spores showing bright fluorescence indicative of high
251 concentrations of YImD or YImE, while others hardly showed any fluorescence (Fig 6A). This
252 suggests that YImD and YImE are differentially expressed throughout the nascent spore chains,

253 and do not exclusively co-localize with FtsZ and the divisome. To rule out possible proteolysis of
254 YlmD- or YlmE-eGFP fusion proteins, Western analysis was performed on extracts of surface-
255 grown *S. coelicolor* mycelia, using antibodies against GFP. *S. coelicolor* M145 with empty vector
256 and *S. coelicolor* M145 expressing freely mobile eGFP⁴¹ were included as controls. Only a single
257 band was identified in strains GAL50 and GAL49, corresponding to the expected lengths for
258 YlmD-eGFP and YlmE-eGFP, respectively (Fig. S3). In both cases, the predicted mass of the fusion
259 protein is around 52 kDa, which conforms well to the apparent mobility seen by Western
260 analysis. The strain expressing only eGFP showed the expected band of around 27 kDa for the
261 non-fused protein. Therefore, we conclude that the observed localizations can indeed be
262 ascribed to intact YlmD- or YlmE-eGFP.

263 The fluorescence intensity of YlmD-eGFP and YlmE-eGFP was measured on images
264 representing different developmental stages (Fig. 6B). As development progressed, the
265 fluorescence intensities increased for both YlmD-eGFP and YlmE-eGFP and reached peak levels
266 during the phase corresponding to late aerial growth and early sporulation. When spores
267 matured, YlmD-eGFP and YlmE-eGFP signals decreased to the level as in vegetative growth.
268 These results suggest YlmD and YlmE proteins are active primarily during the phase of
269 sporulation-specific cell division.

270

271

272 **Localization of FtsZ is disturbed in *yldM* and *yldE* null mutants**

273 To investigate the localization of FtsZ in the mutants, integrative plasmid pKF41 that expresses
274 FtsZ-eGFP from the native *ftsZ* promoter region⁴² was introduced into the *yldM* and *yldE*

275 mutants, to generate strain GAL52 and GAL53, respectively. Prior to sporulation, typical ladders
276 of Z-rings were observed in the parental strain *S. coelicolor* M145, while *ylmD* and *ylmE* null
277 mutants showed abnormal Z-ladders (Fig. 7). In the absence of YlmD, ladders were still observed,
278 but the intensity varied and spacing between the individual rings was less regular, with many
279 neighboring Z-rings either close together or widely spaced. Consistent with the sporulation
280 defect, *ylmE* null mutants produced very few Z-rings, and the few Z-ladders that were formed
281 were highly irregular or unfinished, and significantly shorter than in the parental strain. Thus,
282 FtsZ localization is irregular in *ylmD* mutants and highly compromised in *ylmE* mutants.

283

284 **A model for sporulation control by YlmDE in streptomycetes**

285 Our data show that mutants of *S. coelicolor* lacking *ylmE* have severe developmental defects,
286 with highly compromised cell-wall synthesis and aberrant cell division. Mutants which lack *ylmD*
287 sporulated well, though many spores exhibited aberrant shapes and variable lengths.
288 Surprisingly, the additional deletion of *ylmD* greatly rescued the sporulation-deficient
289 phenotype of *ylmE* mutants, with the *ylmDE* null mutant producing abundant and mostly
290 regularly sized spores.

291 We propose that *YLMD* AND *YLME* Form a two-part system, reminiscent of toxin-
292 antitoxin systems ⁴³. Similarly dysfunction of one protein in the presence of another has also
293 been reported for the sporulation control protein WhiJ, following the observation that media-
294 dependent sporulation defects caused by a point mutation in *whiJ* (SCO4543) could be rescued
295 by the full deletion of *whiJ* ⁴⁴. The authors proposed a model wherein repression of
296 developmental genes by WhiJ could be released when WhiJ interacts with a WhiJ-associated

297 protein encoded by the adjacent gene SCO4542⁴⁴. It was suggested that the aberrant protein
298 WhiJ* still binds to operator sequences of developmental genes, leading to their transcriptional
299 repression, but fails to associate with SCO4542, with a permanent block of transcription of
300 developmental genes as a result⁴⁴. Similarly, the expression of YlmD alone is detrimental for
301 sporulation, suggesting that YlmD acts in a deleterious manner towards sporulation, yet this
302 effect can be relieved by the presence of YlmE. Supporting evidence for this is that deletion of
303 both genes allows *Streptomyces* to develop normally, and by the observation that *ylmD* is never
304 found alone in bacterial genomes, while the occurrence of an orphan *ylmE* is seen frequently.
305 Further support comes from the report that *ylmDE* double mutants of *S. venezuelae* also
306 sporulate relatively normally³². This also indicates that this two-part system functions in a
307 similar manner in a range of *Streptomyces* species. This apparently rules out major divergence
308 between the two morphologically distinct *Streptomyces* clades, namely those that sporulate in
309 submerged cultures and those that do not^{45,46}. However, it will be very interesting to see if
310 submerged sporulation of *S. venezuelae* is prevented by the deletion of just *ylmE*. Currently, we
311 are performing detailed structural and functional analysis of YlmD and YlmE, to elucidate their
312 biochemical function and their precise role in bacterial cell division.

313

314

315 **METHODS**

316 **Phylogenetic analysis of *ylmD* and *ylmE***

317 The amino acid sequence of YlmD and YlmE were extracted from StrepDB
318 (<http://strepdb.streptomyces.org.uk>) and used to search the NCBI database

319 (www.ncbi.nlm.nih.gov) using BLASTP against the non-redundant protein sequence database.
320 Alignment of YlmD and YlmE was generated using ClustalW ⁴⁷ followed by manual editing in
321 MEGA v. 4.0. The neighbour-joining trees ⁴⁸ were generated with default parameters settings as
322 implemented in MEGA v. 4.0 ⁴⁹. The maximum-likelihood trees were made using the best fit
323 models predicted by MEGA. Tree reliability was estimated by bootstrapping with 1000
324 replicates. Trees were drawn with either N-J or ML algorithms gave trees of similar topologies
325 indicating that the phylogenies are likely to reliable.

326

327 **Bacterial strains and media**

328 All bacterial strains used in this study are listed in Table S1. *E. coli* JM109 was used for routine
329 cloning and ET12567 ⁵⁰ to prepare nonmethylated DNA to bypass the methyl-specific restriction
330 system of *S. coelicolor*. *E. coli* strains were propagated in Luria broth, where appropriate
331 supplemented with antibiotics for selection, namely ampicillin (100 µg/ml end concentration),
332 apramycin (50 µg/ml) and/or chloramphenicol (25 µg/ml). *S. coelicolor* A3(2) M145 ⁵¹ and *S.*
333 *lividans* 66 ⁵² were obtained from the John Innes Centre strain collection. *S. coelicolor* strains
334 were grown on soya flour medium (SFM) or minimal media mannitol (MM) agar plates for
335 phenotypic characterization and on R5 agar plates for regeneration of protoplasts ⁵³. Antibiotics
336 used for screening Streptomyces were apramycin (20 µg/ml end concentration) and
337 thiostrepton (10 µg/ml).

338

339 **Plasmids and constructs**

340 All plasmids and constructs described in this study are summarized in Table S2. The
341 oligonucleotides used for PCR are listed in Table S3. PCR reactions were performed using Pfu
342 DNA polymerase as described ⁵⁴. All inserts of the constructs were verified by DNA sequencing,
343 which was performed at BaseClear (Leiden, The Netherlands).

344

345 *Constructs for the deletion of ylmD and ylmE*

346 The strategy for creating knock-out mutants is based on the unstable multi-copy vector pWHD3
347 ⁵⁵ as described previously ⁵⁶. For each knock-out construct roughly 1.5 kb of upstream and
348 downstream region of the respective genes were amplified by PCR from cosmid St4A10 that
349 contains the *dcw* cluster of *S. coelicolor*. The upstream region was thereby cloned as an EcoRI-
350 XbaI fragment, and the downstream part as an XbaI-BamHI fragment, and these were ligated
351 into EcoRI-BamHI-digested pWHD3 (for the precise location of the oligonucleotides see Table
352 S3). In this way, an XbaI site was engineered in-between the flanking regions of the gene of
353 interest. This was then used to insert the apramycin resistance cassette *aac(3)IV* flanked by *loxP*
354 sites, using engineered XbaI sites. The presence of the *loxP* recognition sites allows the efficient
355 removal of the apramycin resistance cassette following the introduction of a plasmid pUWL-Cre
356 expressing the Cre recombinase ^{57,58}. Knock-out plasmids pGWS728 and pGWS729 were created
357 for the deletion of nucleotide positions +25/+696 of *ylmE* (SCO2080) and +25/+705 of *ylmD*
358 (SCO2081), whereby +1 refers to the translational start site of the respective genes. This
359 allowed first the replacement by the apramycin resistance cassette. Subsequently the
360 apramycin resistance cassette was removed using expression of pUWLCre. To create a *ylmDE*
361 double deletion mutant, construct pGWS1044 was created which contains the upstream region

362 of *yImD* and downstream region of *yImE* flanked by *loxP* sites, and with the apramycin
363 resistance cassette *aac(3)IV* inserted in between.

364 For complementation of the *yImE* and *yImD* null mutants, the entire coding regions of
365 SCO2080 and SCO2081 (with stop codons) were amplified from the *S. coelicolor* M145
366 chromosome using primer pairs *yImE_F+1* and *yImE_R+723* and *yImD_F+1* and *yImD_R+732*,
367 respectively. The PCR products were digested with *Sst*I/*Xba*I, and inserted downstream of the
368 native *ftsZ* promoter region in pHJL401, respectively. Thus constructs pGWS1042 and
369 pGWS1043 were generated that express *yImE* and *yImD*, respectively, under control of the *S.*
370 *coelicolor* *ftsZ* promoter region. Alternatively, construct pKR8 was used for complementation;
371 pKR8 is based on integrative vector pIJ8600⁵⁹ and contains the 2227742-2241015 region of the
372 *S. coelicolor* genome, encompassing the end of *murX* (SCO2087), the entire coding sequences of
373 *murD*, *ftsW*, *murG*, *ftsQ*, *ftsZ*, *yImD*, *yImE*, *sepF*, *sepG*, *divIVA* and a large part of SCO2076
374 (encoding Ile-tRNA synthetase).

375

376 *Constructs for the localization of YImD and YImE*

377 The entire coding regions of SCO2080 and SCO2081 (without stop codons) were amplified from
378 the *S. coelicolor* M145 chromosome using primer pairs *yImE_F+1* and *yImE_R+717* and
379 *yImD_F+1* and *yImD_R+726*, respectively. The PCR products were digested with *Sst*I/*Bam*HI, and
380 inserted downstream of the native *ftsZ* promoter region and immediately upstream of *egfp* in
381 pHJL401. The latter is a highly stable vector with low copy number that generally results in wild-
382 type transcription levels and is well suited for among others complementation experiments⁴⁰.
383 Thus constructs pGWS757 and pGWS758 were generated that express YImE-eGFP and YImD-

384 eGFP, respectively, from the native *S. coelicolor ftsZ* promoter region. Plasmid pKF41 expresses
385 FtsZ-eGFP from its own promoter region ⁴². Constructs pGWS757 and pGWS758 were also used
386 to complement *ylmE* and *ylmD* null mutants, respectively.

387

388 **eGFP detection using western blot analysis**

389 Strains were grown on SFM agar plates containing the appropriate antibiotics overlaid with
390 cellophane disks. Biomass (mycelium and spores) was collected after 6 days of growth at 30 °C
391 and suspended in urea lysis buffer (8M urea, 2M thiourea, 4% CHAPS, 1mM PMSF and 65mM
392 DTT), followed by cell disruption via sonication. Western blots were performed as described ⁶⁰.
393 Briefly, cell lysates were obtained after centrifugation at 30,000x g for 30 min at 4°C. Proteins
394 were separated on a 12.5% SDS-PAGE gel, and then transferred to PVDF membrane using Mini
395 Trans-Blot (Bio-Rad). As primary antibody a 1:2000 dilution of GFP antibody (ThermoFisher, REF
396 A11122) was used and incubated for 16 h at 4°C in the presence of 3% BSA. After washing, the
397 membrane was incubated with alkaline phosphatase conjugated anti-rabbit IgG (Sigma) as
398 secondary antibody for 1 h at room temperature. Visualization was done using BCIP/NBT color
399 development substrate.

400

401 **Microscopy**

402 Fluorescence and light microscopy were performed as described previously ⁶¹. For
403 peptidoglycan staining we used FITC-labeled wheat germ agglutinin (FITC-WGA) or Oregon
404 Green 488 conjugated WGA (Oregon-WGA); for membrane staining, we used FM5-95 (all
405 obtained from Molecular Probes). All images were background-corrected, setting the signal

406 outside the hyphae to 0 to obtain a sufficiently dark background. These corrections were
407 made using Adobe Photoshop CS4. Cryo-scanning electron microscopy (cryo-SEM) and
408 transmission electron microscopy (TEM) were performed as described ⁶². For quantification of
409 fluorescence intensity of YlmD-eGFP and YlmE-eGFP, the arbitrary average intensity values of
410 manually selected areas of interest were determined as relative fluorescence intensity. All green
411 fluorescent images were made with equal exposure time.

412

413 **Data analysis**

414 For the Kolmogorov–Smirnov (KS) test, the critical value D_{crit} was calculated for the number of
415 measured spores (n) and significance level (α) of 0.05: $D_{crit} = \sqrt{\frac{-0.5 * \ln(\frac{\alpha}{2})}{\sqrt{n}}}$. The difference (D_n)
416 between the observed cumulative distribution function (F_{obs}) and the expected cumulative
417 distribution function (F_{exp}) was calculated as: $D_n = |F_{exp}(x) - F_{obs}(x)|$. The maximal value was
418 identified as D_{max} . The null hypothesis that the data comes from the specified distribution was
419 rejected if $D_{max} > D_{crit}$. The Mann-Whitney U test was done using the SPSS software release 24.0.

420

421 **Computer analysis**

422 DNA and protein database searches were completed by using StrepDB
423 (<http://strepdb.streptomyces.org.uk/>). Phylogenetic analysis was done using the STRING engine
424 at EMBL (www.string.EMBL).

425

426 **DATA AVAILABILITY**

427 All strains, materials and data will be made available upon request.

428

429 **ACKNOWLEDGEMENTS**

430 This work was supported by the Netherlands Organization for Scientific Research (NWO), via

431 VICI grant 10379 to GPvW.

432

433 **COMPETING FINANCIAL INTERESTS**

434 The authors declare no conflict of interests.

435

436 **AUTHOR CONTRIBUTIONS**

437 LZ performed the molecular biology experiments and created the mutants and expression

438 constructs, JW performed the imaging and PAH the phylogenetic analysis. GVW conceived the

439 experiments together with the other authors. All authors wrote and approved the manuscript.

440

441 **REFERENCES**

442 1 Bi, E. F. & Lutkenhaus, J. FtsZ ring structure associated with division in *Escherichia coli*.
443 *Nature* **354**, 161-164 (1991).

444 2 Goehring, N. W. & Beckwith, J. Diverse paths to midcell: assembly of the bacterial cell
445 division machinery. *Curr Biol* **15**, R514-526 (2005).

446 3 Adams, D. W. & Errington, J. Bacterial cell division: assembly, maintenance and
447 disassembly of the Z ring. *Nat Rev Microbiol* **7**, 642-653 (2009).

448 4 Hale, C. A. & de Boer, P. A. J. Direct Binding of FtsZ to ZipA, an essential component of
449 the septal ring structure that mediates cell division in *E. coli*. *Cell* **88**, 175-185 (1997).

450 5 RayChaudhuri, D. ZipA is a MAP-Tau homolog and is essential for structural integrity of
451 the cytokinetic FtsZ ring during bacterial cell division. *EMBO J* **18**, 2372-2383 (1999).

452 6 Sekine, H., Mimura, J., Yamamoto, M. & Fujii-Kuriyama, Y. Unique and overlapping
453 transcriptional roles of arylhydrocarbon receptor nuclear translocator (Arnt) and Arnt2
454 in xenobiotic and hypoxic responses. *J Biol Chem* **281**, 37507-37516 (2006).

455 7 Gueiros-Filho, F. J. & Losick, R. A widely conserved bacterial cell division protein that
456 promotes assembly of the tubulin-like protein FtsZ. *Genes Dev* **16**, 2544-2556 (2002).

457 8 Hamoen, L. W., Meile, J. C., de Jong, W., Noirot, P. & Errington, J. SepF, a novel FtsZ-
458 interacting protein required for a late step in cell division. *Mol Microbiol* **59**, 989-999
459 (2006).

460 9 Ishikawa, S., Kawai, Y., Hiramatsu, K., Kuwano, M. & Ogasawara, N. A new FtsZ-
461 interacting protein, YlmF, complements the activity of FtsA during progression of cell
462 division in *Bacillus subtilis*. *Mol Microbiol* **60**, 1364-1380 (2006).

463 10 Romberg, L. & Levin, P. A. Assembly dynamics of the bacterial cell division protein FTSZ:
464 poised at the edge of stability. *Annu Rev Microbiol* **57**, 125-154 (2003).

465 11 Barka, E. A. *et al.* Taxonomy, physiology, and natural products of the *Actinobacteria*.
466 *Microbiol Mol Biol Rev* **80**, 1-43 (2016).

467 12 Hopwood, D. A. *Streptomyces in nature and medicine: the antibiotic makers*. (Oxford
468 University Press, 2007).

469 13 Wildermuth, H. & Hopwood, D. Septation during sporulation in *Streptomyces coelicolor*. *J
470 Gen Microbiol* **60**, 51-59 (1970).

471 14 Claessen, D., Rozen, D. E., Kuipers, O. P., Sogaard-Andersen, L. & van Wezel, G. P.
472 Bacterial solutions to multicellularity: a tale of biofilms, filaments and fruiting bodies.
473 *Nat Rev Microbiol* **12**, 115-124 (2014).

474 15 Flärdh, K. & Buttner, M. J. *Streptomyces* morphogenetics: dissecting differentiation in a
475 filamentous bacterium. *Nat Rev Microbiol* **7**, 36-49 (2009).

476 16 McCormick, J. R. Cell division is dispensable but not irrelevant in *Streptomyces*. *Curr Opin
477 Microbiol* **12**, 689-698 (2009).

478 17 Celler, K., Koning, R. I., Willemse, J., Koster, A. J. & van Wezel, G. P. Cross-membranes
479 orchestrate compartmentalization and morphogenesis in *Streptomyces*. *Nat Comms* **7**,
480 11836 (2016).

481 18 Yague, P. *et al.* Subcompartmentalization by cross-membranes during early growth of
482 *Streptomyces* hyphae. *Nat Comms* **7**, 12467 (2016).

483 19 Holmes, N. A. *et al.* Coiled-coil protein Scy is a key component of a multiprotein
484 assembly controlling polarized growth in *Streptomyces*. *Proc Natl Acad Sci U S A* **110**,
485 E397-406 (2013).

486 20 Celler, K., Koning, R. I., Koster, A. J. & van Wezel, G. P. Multidimensional view of the
487 bacterial cytoskeleton. *J Bacteriol* **195**, 1627-1636 (2013).

488 21 Jakimowicz, D. & van Wezel, G. P. Cell division and DNA segregation in *Streptomyces*:
489 how to build a septum in the middle of nowhere? *Mol Microbiol* **85**, 393-404 (2012).

490 22 Schwedock, J., McCormick, J. R., Angert, E. R., Nodwell, J. R. & Losick, R. Assembly of the
491 cell division protein FtsZ into ladder like structures in the aerial hyphae of *Streptomyces*
492 *coelicolor*. *Mol Microbiol* **25**, 847-858 (1997).

493 23 McCormick, J. R., Su, E. P., Driks, a. & Losick, R. Growth and viability of *Streptomyces*
494 *coelicolor* mutant for the cell division gene *ftsZ*. *Mol Microbiol* **14**, 243-254 (1994).

495 24 McCormick, J. R. & Losick, R. Cell division gene *ftsQ* is required for efficient sporulation
496 but not growth and viability in *Streptomyces coelicolor* A3(2). *J Bacteriol* **178**, 5295-5301
497 (1996).

498 25 Traag, B. A. & van Wezel, G. P. The SsgA-like proteins in actinomycetes: small proteins up
499 to a big task. *Antonie Van Leeuwenhoek* **94**, 85-97 (2008).

500 26 Girard, G. *et al.* A novel taxonomic marker that discriminates between morphologically
501 complex actinomycetes. *Open Biol* **3**, 130073 (2013).

502 27 Willemse, J., Borst, J. W., de Waal, E., Bisseling, T. & van Wezel, G. P. Positive control of
503 cell division: FtsZ is recruited by SsgB during sporulation of *Streptomyces*. *Genes Dev* **25**,
504 89-99 (2011).

505 28 Keijser, B. J., Noens, E. E., Kraal, B., Koerten, H. K. & van Wezel, G. P. The *Streptomyces*
506 *coelicolor* *ssgB* gene is required for early stages of sporulation. *FEMS Microbiol Lett* **225**,
507 59-67 (2003).

508 29 van Wezel, G. P. *et al.* *ssgA* is essential for sporulation of *Streptomyces coelicolor* A3(2)
509 and affects hyphal development by stimulating septum formation. *J Bacteriol* **182**, 5653-
510 5662 (2000).

511 30 Zhang, L., Willemse, J., Claessen, D. & van Wezel, G. P. SepG coordinates sporulation-
512 specific cell division and nucleoid organization in *Streptomyces coelicolor*. *Open Biol* **6**,
513 150164 (2016).

514 31 Mingorance, J., Tamames, J. & Vicente, M. Genomic channeling in bacterial cell division. *J*
515 *Mol Recognit* **17**, 481-487 (2004).

516 32 Santos-Benit, F., Gu, J. Y., Stimming, U. & Errington, J. *yImD* and *yImE* genes are
517 dispensable for growth, cross-wall formation and sporulation in *Streptomyces*
518 *venezuelae*. *Heliyon* **3**, e00459 (2017).

519 33 Romero, D. A. *et al.* A comparison of key aspects of gene regulation in *Streptomyces*
520 *coelicolor* and *Escherichia coli* using nucleotide-resolution transcription maps produced
521 in parallel by global and differential RNA sequencing. *Mol Microbiol* **94**, 963-987 (2014).

522 34 Swiatek, M. A. *et al.* The ROK family regulator RokB7 pleiotropically affects xylose
523 utilization, carbon catabolite repression, and antibiotic production in *Streptomyces*
524 *coelicolor*. *J Bacteriol* **195**, 1236-1248 (2013).

525 35 Szklarczyk, D. *et al.* The STRING database in 2011: functional interaction networks of
526 proteins, globally integrated and scored. *Nucleic Acids Res* **39**, D561-D568 (2011).

527 36 Claus, H. Laccases and their occurrence in prokaryotes. *Arch Microbiol* **179**, 145-150
528 (2003).

529 37 Eswaramoorthy, S. *et al.* Structure of a yeast hypothetical protein selected by a
530 structural genomics approach. *Acta Crystallogr D Biol Crystallogr* **59**, 127-135 (2002).

531 38 Percudani, R. & Peracchi, A. A genomic overview of pyridoxal-phosphate-dependent
532 enzymes. *EMBO R* **4**, 850-854 (2003).

533 39 Tassoni, R., van der Aart, L. T., Ubbink, M., van Wezel, G. P. & Pannu, N. S. Structural and
534 functional characterization of the alanine racemase from *Streptomyces coelicolor* A3(2).
535 *Biochem Biophys Res Comm* **483**, 122-128 (2017).

536 40 van Wezel, G. P., White, J., Hoogvliet, G. & Bibb, M. J. Application of *redD*, the
537 transcriptional activator gene of the undecylprodigiosin biosynthetic pathway, as a
538 reporter for transcriptional activity in *Streptomyces coelicolor* A3(2) and *Streptomyces*
539 *lividans*. *J Mol Microbiol Biotechnol* **2**, 551-556. (2000).

540 41 Zucchetti, B. *et al.* Aggregation of germlings is a major contributing factor towards
541 mycelial heterogeneity of *Streptomyces*. *Sci Rep* **6**, 27045 (2016).

542 42 Grantcharova, N., Lustig, U. & Flärdh, K. Dynamics of FtsZ assembly during sporulation in
543 *Streptomyces coelicolor* A3(2). *J Bacteriol* **187**, 3227-3237 (2005).

544 43 Yamaguchi, Y., Park, J. H. & Inouye, M. Toxin-antitoxin systems in bacteria and archaea.
545 *Ann Rev Genet* **45**, 61-79 (2011).

546 44 Ainsa, J. A., Bird, N., Ryding, N. J., Findlay, K. C. & Chater, K. F. The complex *whiJ* locus
547 mediates environmentally sensitive repression of development of *Streptomyces*
548 *coelicolor* A3(2). *Antonie Van Leeuwenhoek* **98**, 225-236 (2010).

549 45 Girard, G. *et al.* A novel taxonomic marker that discriminates between morphologically
550 complex actinomycetes. *Open Biol* **3**, 130073 (2013).

551 46 van Dissel, D., Claessen, D. & Van Wezel, G. P. Morphogenesis of *Streptomyces* in
552 submerged cultures. *Adv Appl Microbiol* **89**, 1-45 (2014).

553 47 Thompson, J. D., Higgins, D. G. & Gibson, T. J. Clustal-W: improving the sensitivity of
554 progressive multiple sequence alignment through sequence weighting, position-specific
555 gap penalties and weight matrix choice. *Nucleic Acids Res* **22**, 4673-4680 (1994).

556 48 Saitou, N. & Nei, M. The neighbor-joining method: a new method for reconstructing
557 phylogenetic trees. *Mol Biol Evol* **4**, 406-425 (1987).

558 49 Tamura, K., Dudley, J., Nei, M. & Kumar, S. MEGA4: Molecular Evolutionary Genetics
559 Analysis (MEGA) software version 4.0. *Mol Biol Evol* **24**, 1596-1599 (2007).

560 50 MacNeil, D. J. *et al.* Analysis of *Streptomyces avermitilis* genes required for avermectin
561 biosynthesis utilizing a novel integration vector. *Gene* **111**, 61-68 (1992).

562 51 Bentley, S. D. *et al.* Complete genome sequence of the model actinomycete
563 *Streptomyces coelicolor* A3(2). *Nature* **417**, 141-147 (2002).

564 52 Cruz-Morales, P. *et al.* The genome sequence of *Streptomyces lividans* 66 reveals a novel
565 tRNA-dependent peptide biosynthetic system within a metal-related genomic island.
566 *Genome Biol Evol* **5**, 1165-1175 (2013).

567 53 Kieser, T., Bibb, M. J., Buttner, M. J., Chater, K. F. & Hopwood, D. A. *Practical*
568 *Streptomyces genetics*. (John Innes Foundation, 2000).

569 54 Colson, S. *et al.* Conserved *cis*-acting elements upstream of genes composing the
570 chitinolytic system of streptomycetes are DasR-responsive elements. *J Mol Microbiol*
571 *Biotechnol* **12**, 60-66 (2007).

572 55 Vara, J., Lewandowska-Skarbek, M., Wang, Y. G., Donadio, S. & Hutchinson, C. R. Cloning
573 of genes governing the deoxysugar portion of the erythromycin biosynthesis pathway in
574 *Saccharopolyspora erythraea* (*Streptomyces erythreus*). *J Bacteriol* **171**, 5872-5881
575 (1989).

576 56 Świątek, M. A., Tenconi, E., Rigali, S. & van Wezel, G. P. Functional analysis of the N-
577 acetylglucosamine metabolic genes of *Streptomyces coelicolor* and role in control of
578 development and antibiotic production. *J Bacteriol* **194**, 1136-1144 (2012).

579 57 Fedoryshyn, M., Welle, E., Bechthold, A. & Luzhetsky, A. Functional expression of the
580 Cre recombinase in actinomycetes. *App Microbiol Biotechnol* **78**, 1065-1070 (2008).

581 58 Khodakaramian, G. *et al.* Expression of Cre recombinase during transient phage infection
582 permits efficient marker removal in *Streptomyces*. *Nucleic Acids Res* **34**, e20 (2006).

583 59 Sun, J., Kelemen, G. H., Fernandez-Abalos, J. M. & Bibb, M. J. Green fluorescent protein
584 as a reporter for spatial and temporal gene expression in *Streptomyces coelicolor* A3(2).
585 *Microbiology* **145**, 2221-2227 (1999).

586 60 Vijgenboom, E. *et al.* Three *tuf*-like genes in the kirromycin producer *Streptomyces*
587 *ramocissimus*. *Microbiology* **140**, 983-998 (1994).

588 61 Willemse, J. & van Wezel, G. P. Imaging of *Streptomyces coelicolor* A3(2) with Reduced
589 Autofluorescence Reveals a Novel Stage of FtsZ Localization. *PLoS ONE* **4**, e4242 (2009).

590 62 Piette, A. *et al.* From dormant to germinating spores of *Streptomyces coelicolor* A3(2):
591 new perspectives from the *crp* null mutant. *J Proteome Res* **4**, 1699-1708 (2005).

592
593

FIGURE LEGENDS

Figure 1. Phylogenetic analysis of YlmE in actinobacteria and its genetic linkage to *yImD*. A phylogenetic tree is shown of YlmE in actinobacteria (left) and genetic linkage of *yImE* (grey) to *ftsZ* (black) and *yImD* (white) (right).

Figure 2. Phenotype of the *S. coelicolor* *yImD* and *yImE* mutants. (A) sporulation of *S. coelicolor* M145 and its *yImD*, *yImE* and *yImDE* mutants on SFM agar after 5 days incubation. Note the lack of grey pigmentation of the *yImE* mutant, indicative of a sporulation defect. (B) phase-contrast micrographs of impression prints of the strains shown in (A) as well as the complemented mutants. Arrows point at irregularly shaped spores in the *yImD* mutant. The sporulation defect of the *yImD* mutant could be complemented by introduction of wild-type *yImD* and *yImD-eGFP*, while complementation of the *yImE* mutant by wild-type *yImE* or *yImE-egfp* restored sporulation, although irregularly sized spores were often produced. Full complementation of *yImE* mutants was obtained by introduction of pKR8, which contains part of the *S. coelicolor* *dcw* cluster. Bar, 5 μ m. (C) Size distributions of wild-type spores and those of *yImD*, *yImE* and *yImDE* mutants presented as boxplots. Data are presented as median and interquartile range in boxplots, with whiskers spread to the maximal and minimal values. The numbers (n) of spores measured for each strain are indicated. Assessment of normality of spore length data was performed by a Kolgomorov-Smirnov test, the results showing that spore length data for all mutants followed non-normal distribution ($D_{\max} > D_{\text{crit}}$). The shown two-tailed P values between each mutant and the parental strain were calculated using a Mann-Whitney U test. The two-tailed P values were

far below 0.05, which shows that the sizes of the mutant spores deviated significantly from those of wild-type spores.

Figure 3. Cryo-scanning electron micrographs of aerial hyphae of *S. coelicolor* M145 and its *yldM* and *yldE* mutants. The parental strain produced wild-type spores, the *yldM* mutant produced abundant but often irregular spores, while the *yldE* null mutant produced occasional spores with highly irregular sizes. Cultures were grown on SFM agar plates for 5 days at 30⁰C. Bars: top row, 1 μ m; bottom row, 5 μ m.

Figure 4. Transmission electron micrographs of spores of *S. coelicolor* M145 and its *yldM* and *yldE* mutants. Wild-type spores (M145) show regular sizes and appearance (A). In contrast, spores of the *yldM* (B) and *yldE* (C) null mutants have an irregular appearance. Note the lighter appearance of the spore wall in the *yldM* null mutant and the lack of the typical thick spore wall in *yldE* mutants. Cultures were grown on SFM agar plates for 5 days at 30⁰C. Bar, 500 nm.

Figure 5. Fluorescence microscopy of cell wall, DNA and membranes.

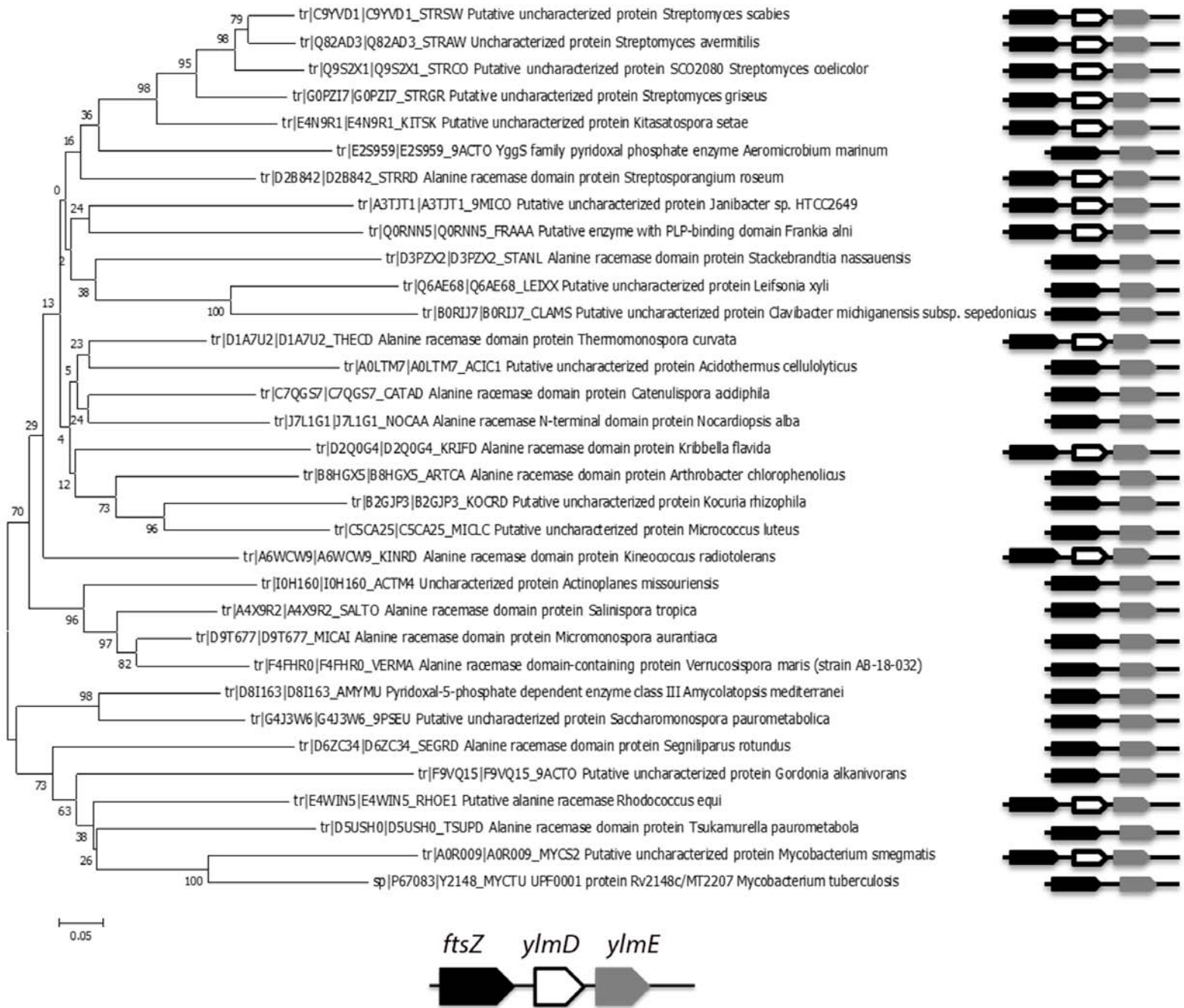
(A) Fluorescent micrographs of hyphae stained for cell-wall synthesis (FITC-WGA or Oregon-WGA) or membranes (FM5-95). An overlay of these images is presented in the third column, and the corresponding light image in the last column. Bar, 5 μ m. (B) Fluorescence micrographs showing DNA and cell-wall distribution in the complemented *yldM* and *yldE* mutants. While ladders of septa were formed in both strains, indicative that sporulation was restored to the

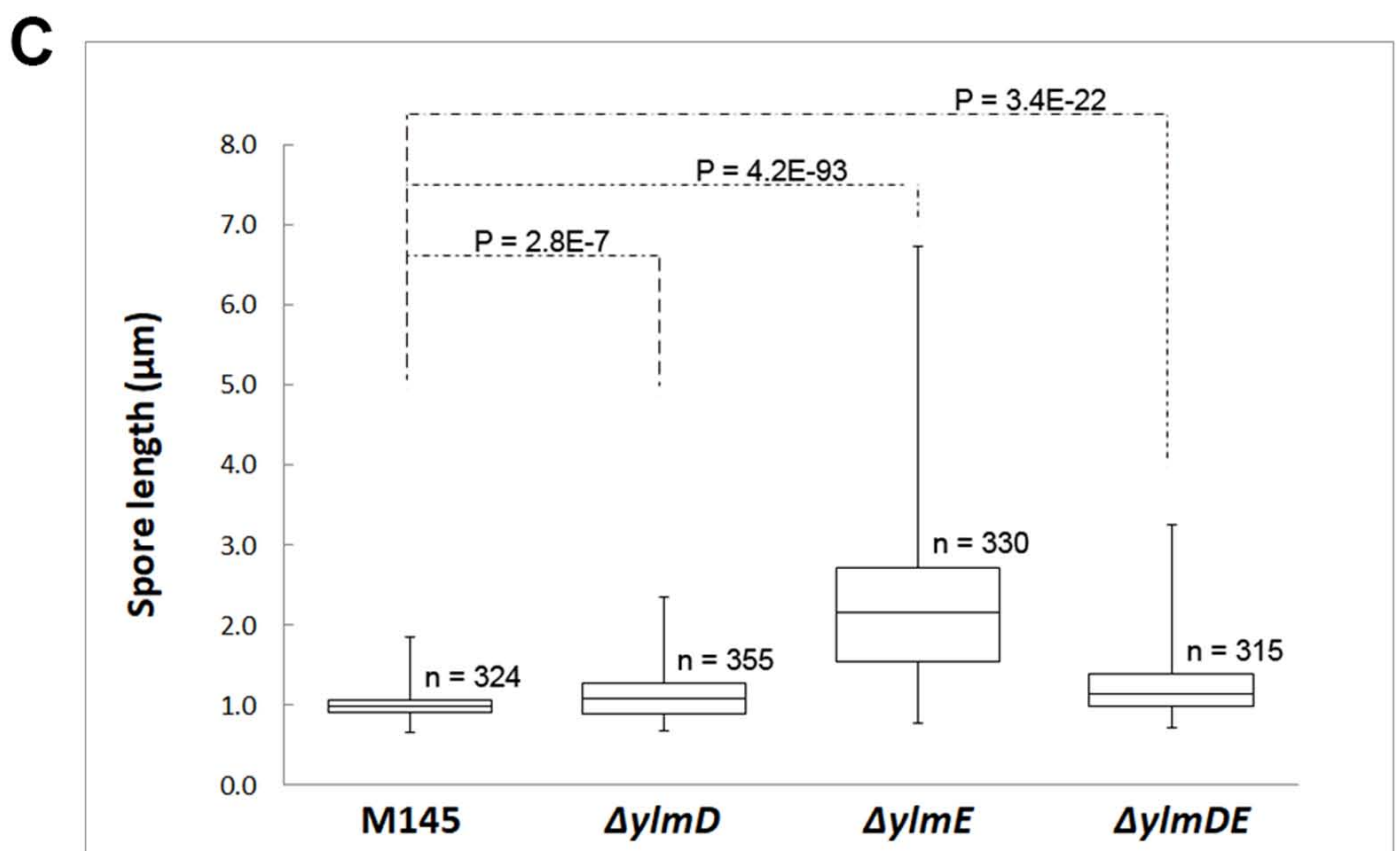
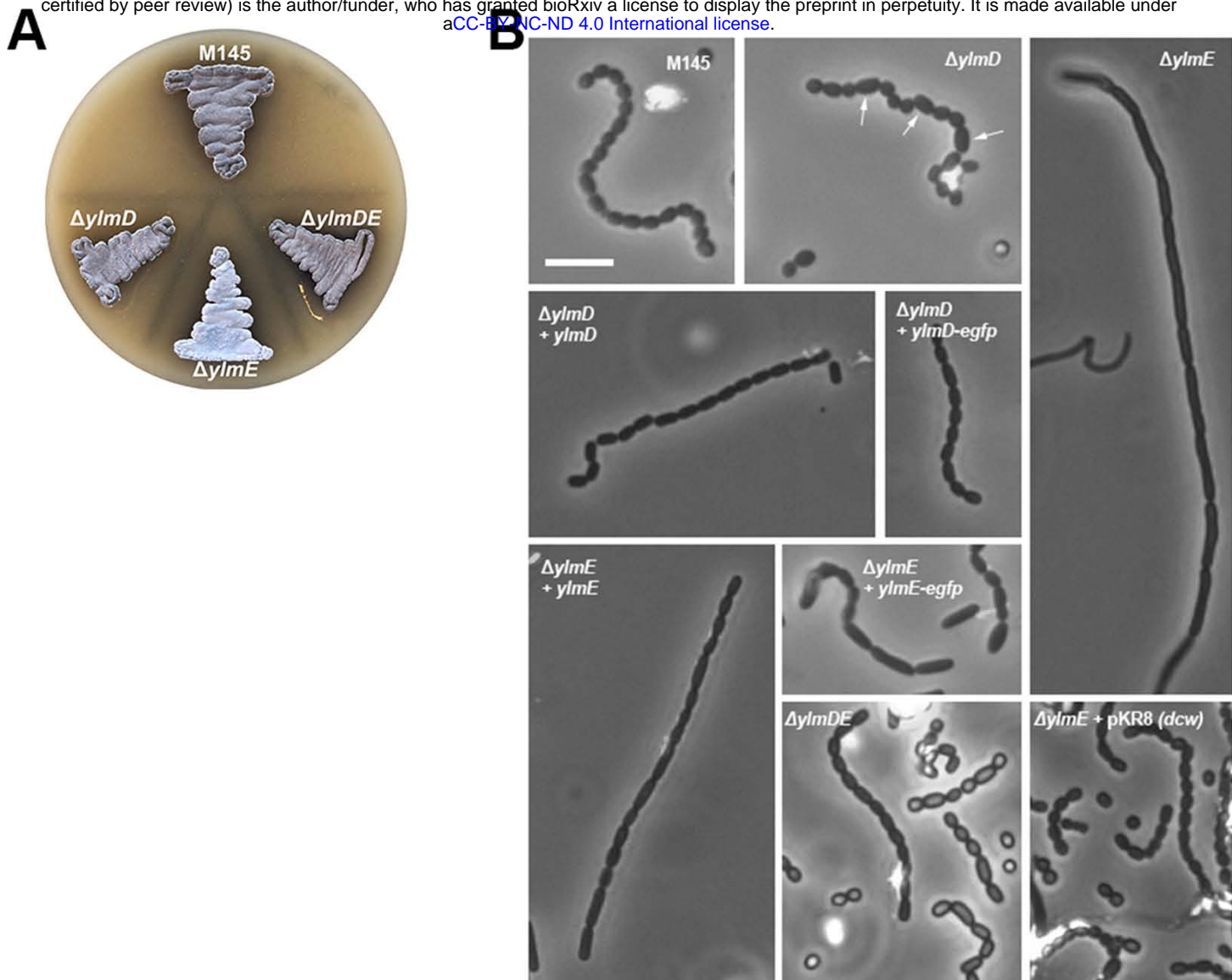
mutants, in particular the complemented *yImE* mutant formed imperfect septa. Cultures were grown on SFM agar plates for 5 days at 30⁰C. Bar, 10 µm.

Figure 6. Localization of YImD-GFP and YImE-GFP.

(A) Sporogenic aerial hyphae of *S. coelicolor* M145 at different stages of development were imaged by fluorescence microscopy visualizing YImD-eGFP and YImE-eGFP. Stages were: vegetative growth, early aerial development, late aerial development, early sporulation and mature spores. During spore maturation, YImD and YImE had a 'patchy' localization, suggesting that at this stage YImD and YImE may co-localize with the cell-wall synthetic machinery. Bar, 5 µm. (B) Relative fluorescence intensity of YImD-eGFP and YImE-eGFP during *Streptomyces* development. VEG, vegetative growth; EA, early aerial growth; LA, late aerial growth; ES, early sporulation; MS, mature spores.

Figure 7. Localization of FtsZ-eGFP in *S. coelicolor* M145 and its *yImD* and *yImE* mutants. FtsZ-eGFP formed typical ladders in wild-type cells (M145). In contrast, YImE is required for the formation of ladders of FtsZ, while the absence of YImD caused irregular spacing between the septa. Cultures were grown on SFM agar plates for 5 days at 30⁰C. Bar, 5 µm.

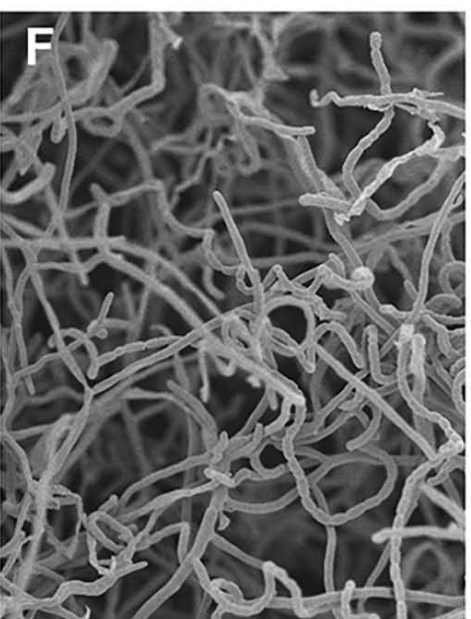
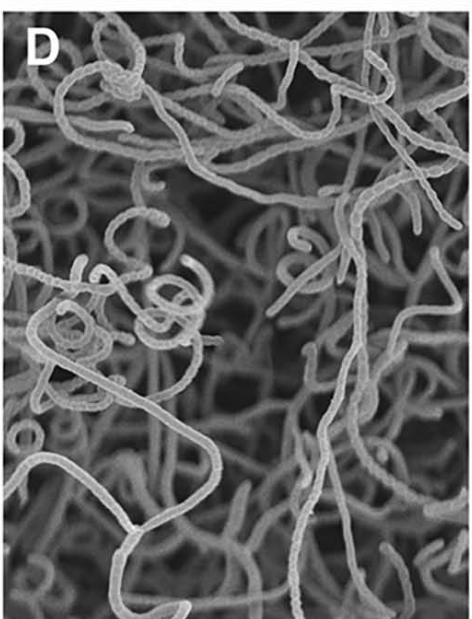
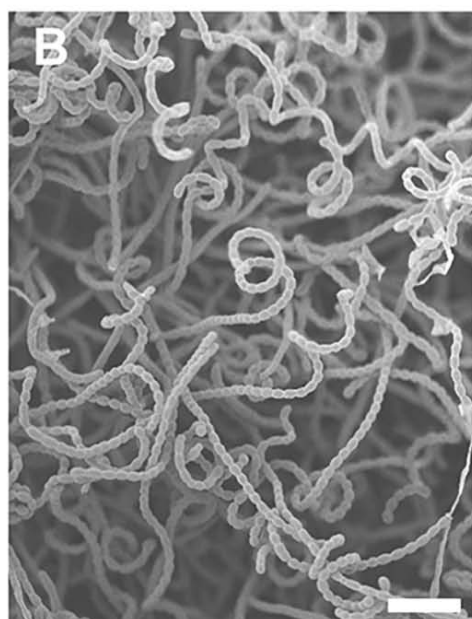
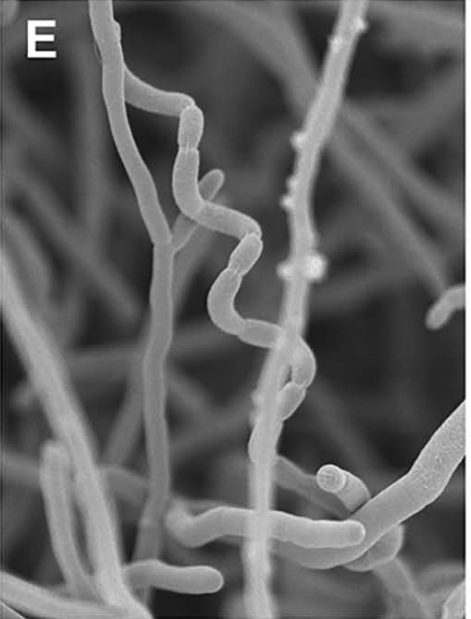
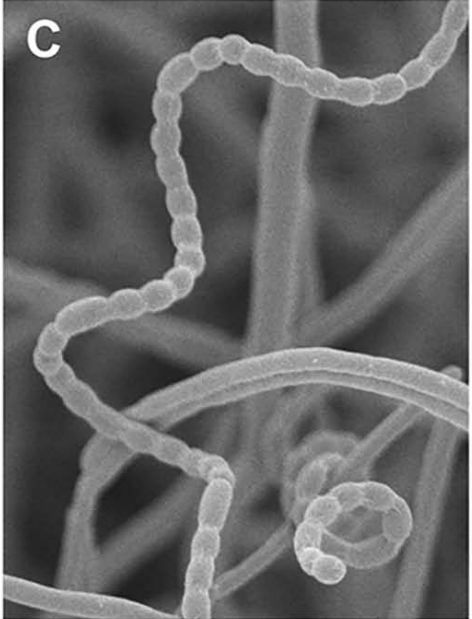
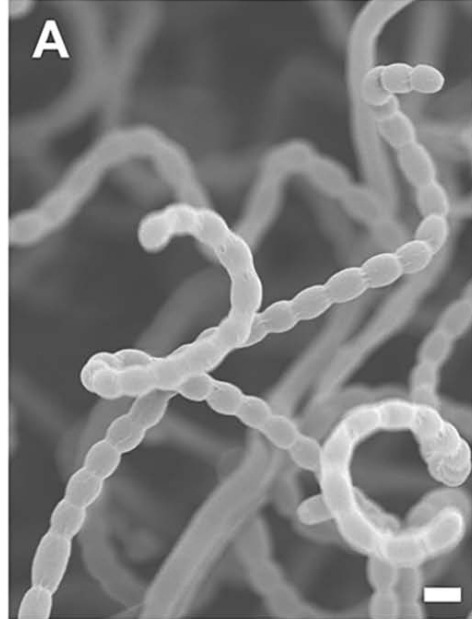




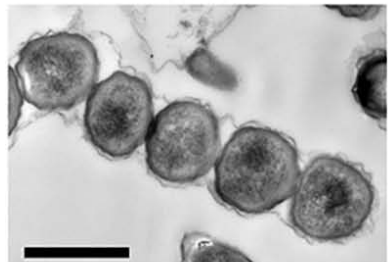
M145

$\Delta ylmD$

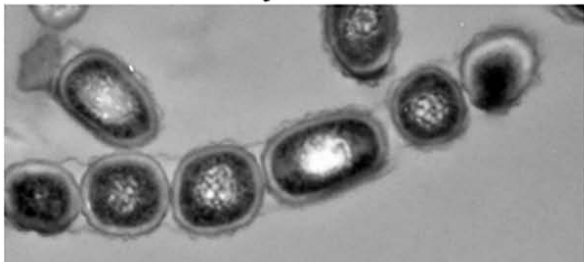
$\Delta ylmE$



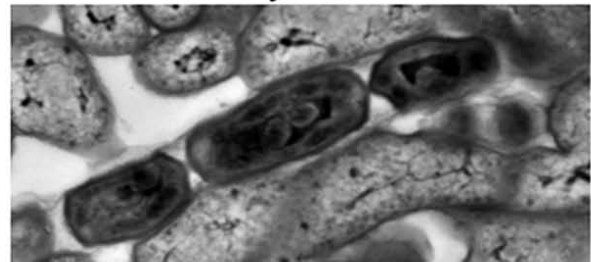
M145

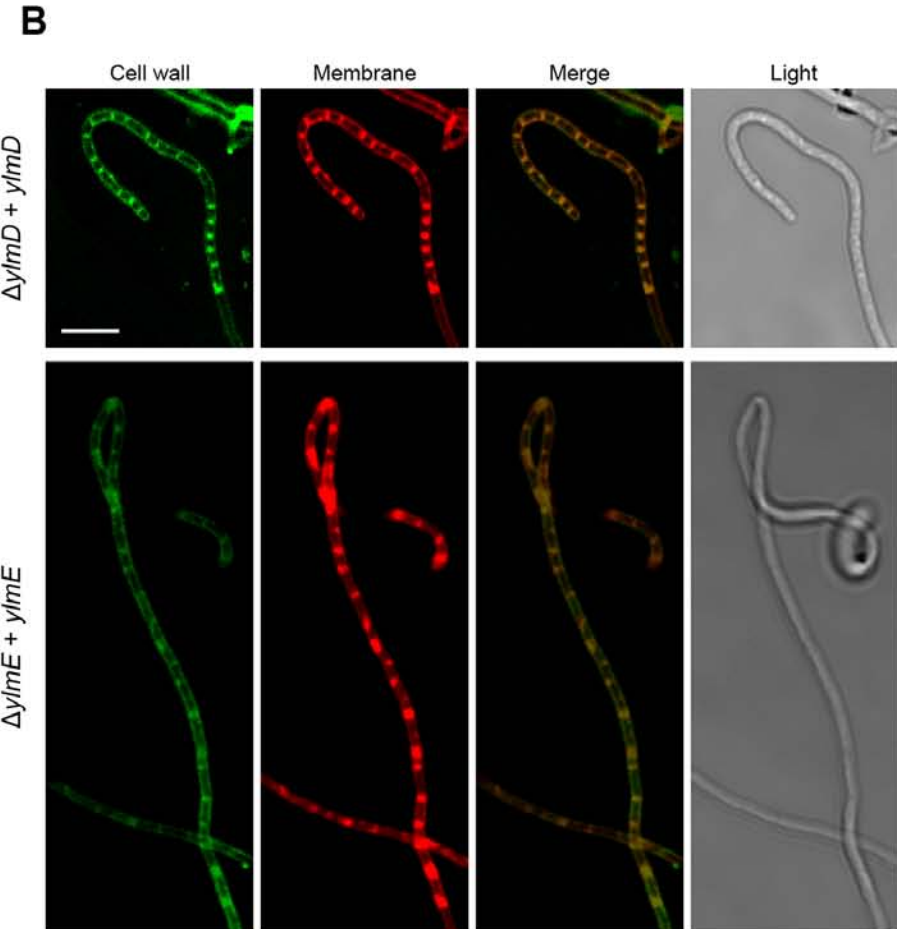
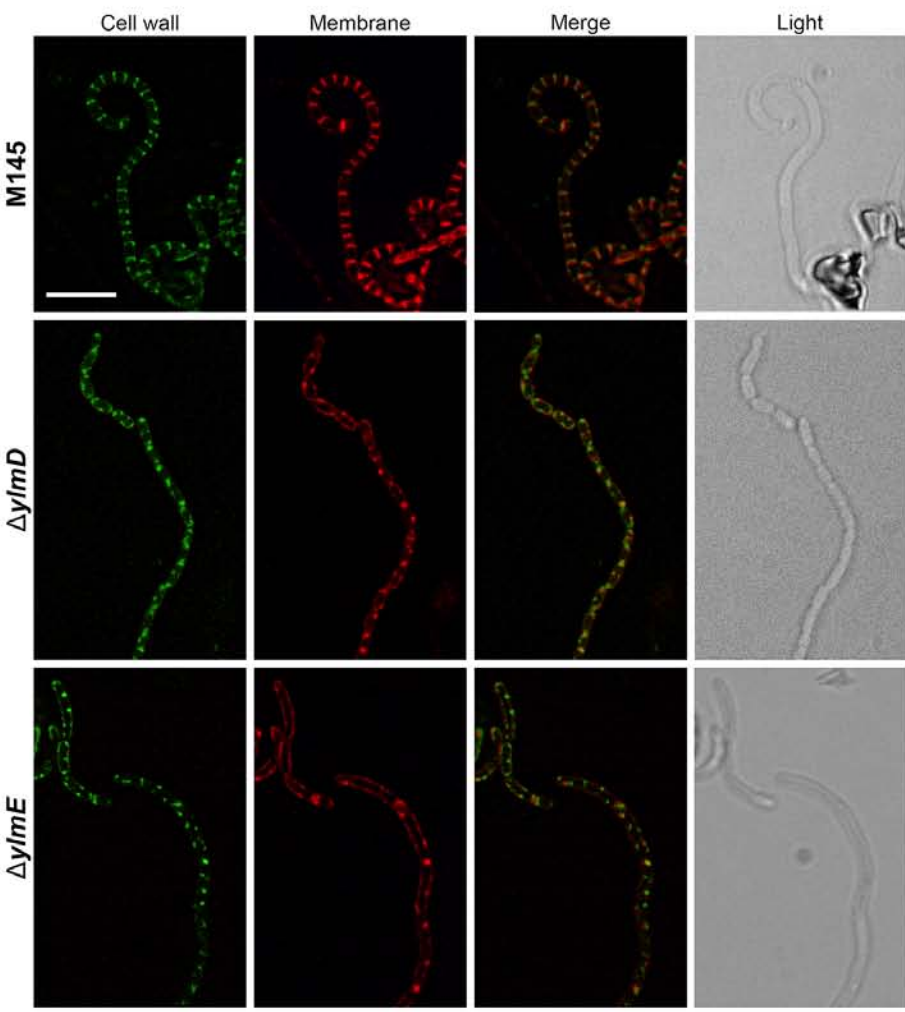


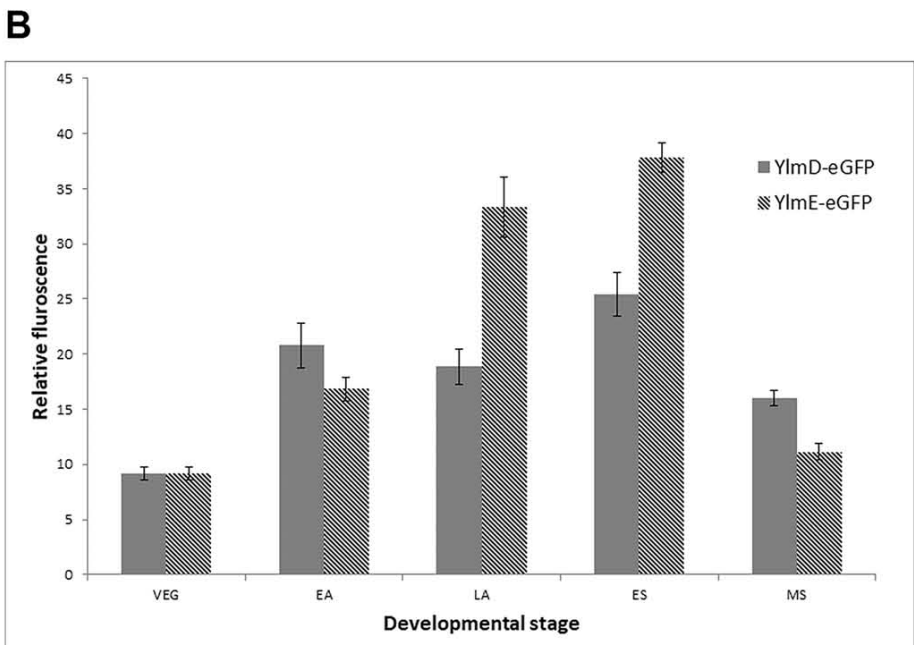
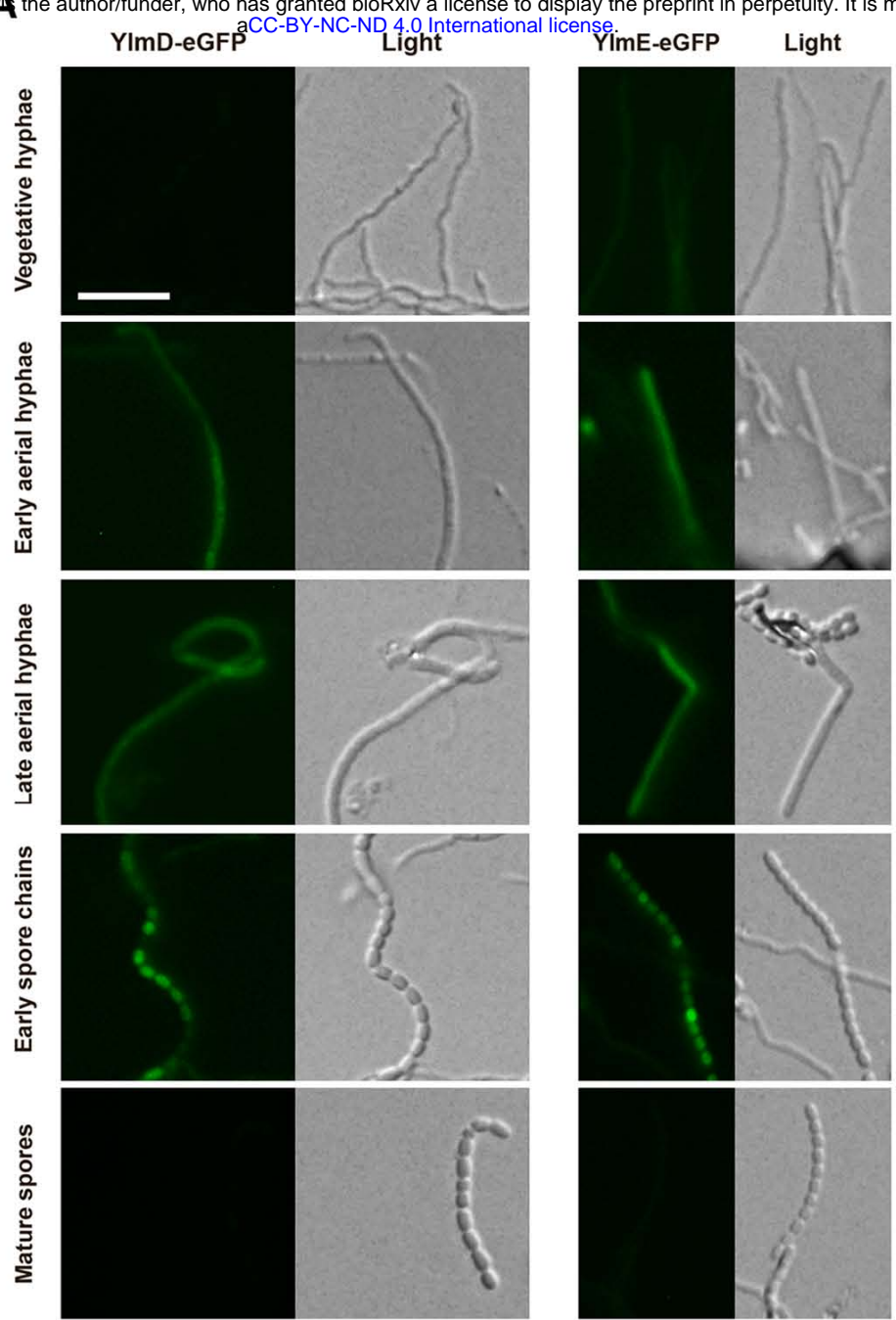
$\Delta ylmD$



$\Delta ylmE$







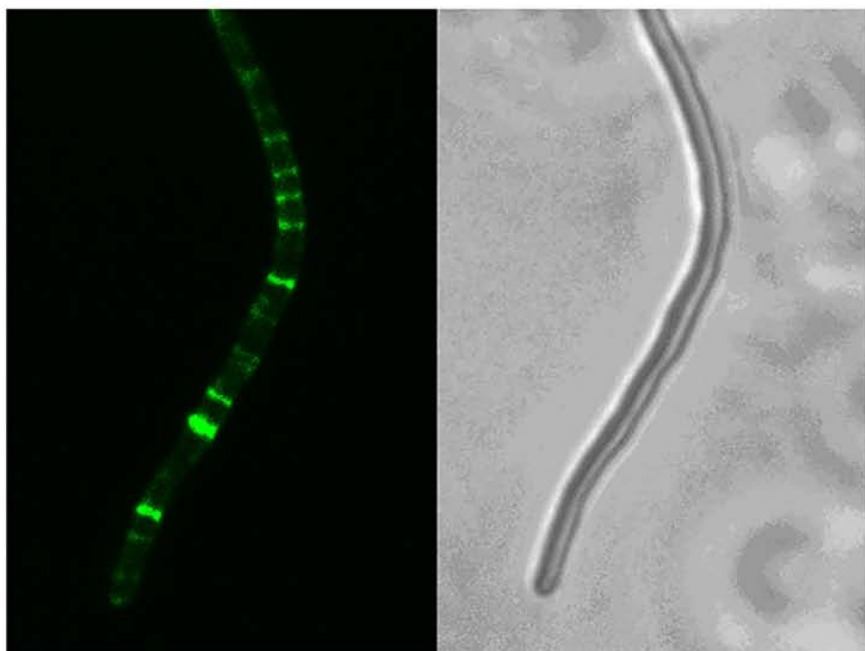
FtsZ-eGFP

Light

M145



$\Delta ylmD$



$\Delta ylmE$

